

# Small-Footprint, High-Efficiency, Integrated Transmitters for High-Speed Optical Interconnect Applications

Erik J. Skogen<sup>†</sup>, Chad S. Wang<sup>†</sup>, James W. Raring<sup>\*</sup>, Gordon B. Morrison<sup>†</sup>, and Larry A. Coldren<sup>†\*</sup>

<sup>†</sup>ECE Dept. University of California, Santa Barbara, CA 93106

<sup>\*</sup>Materials Dept. University of California, Santa Barbara, CA 93106

Phone: 805.893.8465, Fax: 805.893.4500, Email: skogen@engineering.ucsb.edu

**Abstract:** Short-cavity InGaAsP/InP DBR lasers with integrated SOA and EAM were fabricated using a quantum well intermixing processing platform. >10mW output power and 17.5% wall-plug efficiency was achieved at 30mA. EAM extinction was >15dB at -4V.

©2004 Optical Society of America

OCIS codes: (140.5960) Semiconductor lasers; (250.5300) Photonic Integrated Circuits

## 1. INTRODUCTION

Chip to chip optical interconnects (C2OI) have the potential to demonstrate numerous advantages over traditional electrical I/O integrated circuits. Applications requiring high bandwidth-path length products will be best served through an optical free-space type interconnect [1]. This technology will also lead to advantages in power dissipation, crosstalk, and susceptibility to electro-magnetic interference (EMI) than electrical connections.

In order to meet and exceed existing electrical I/O specifications, it is necessary to design and develop short cavity lasers with a small footprint (< 250  $\mu\text{m}$  pitch), high efficiency, low power dissipation, and high output power. Here we demonstrate a short cavity, high output power, single mode, high efficiency, distributed Bragg reflector (DBR) laser, with monolithically integrated semiconductor optical amplifier (SOA) and electro-absorption modulator (EAM).

## 2. EXPERIMENT

The short-cavity DBR lasers were designed to have a high-reflectivity (HR) rear mirror, short gain section (150  $\mu\text{m}$ ), and front DBR mirror (40  $\mu\text{m}$ ). The DBR lasers were monolithically integrated with an SOA (110  $\mu\text{m}$ ) and EAMs (125  $\mu\text{m}$ ) using a quantum well intermixing processing platform that allows for the formation of a unique quantum well band edge for each integrated component. In this device architecture, two modulators with differing band-edge placement were included, one at the passive waveguide band-edge (M1), and one at the EAM band-edge (M2). A side-view schematic of the device and an electron micrograph are shown in Fig. 1a and 1b, respectively.

With this process it is possible to achieve any number of band-edges across the wafer, limited only by the practical number of lithographic process steps as shown in Fig. 2a and 2b. For this work, only three band-edges were needed: the as grown band-edge for the gain regions, a band-edge ideal for the EAM, and a band-edge used in the low loss passive waveguide regions. The photoluminescence curves for sample used in this work are shown in Fig. 2c.

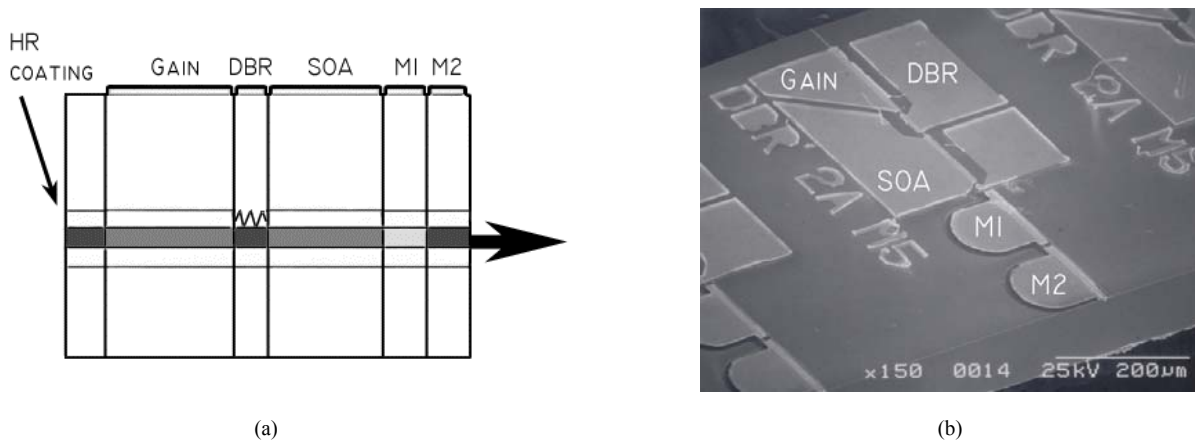


**FIGURE 1.** (a) Side view schematic and (b) electron micrograph of the completed short-cavity DBR laser, illustrating the Gain, DBR, SOA, and 2 section EAM.

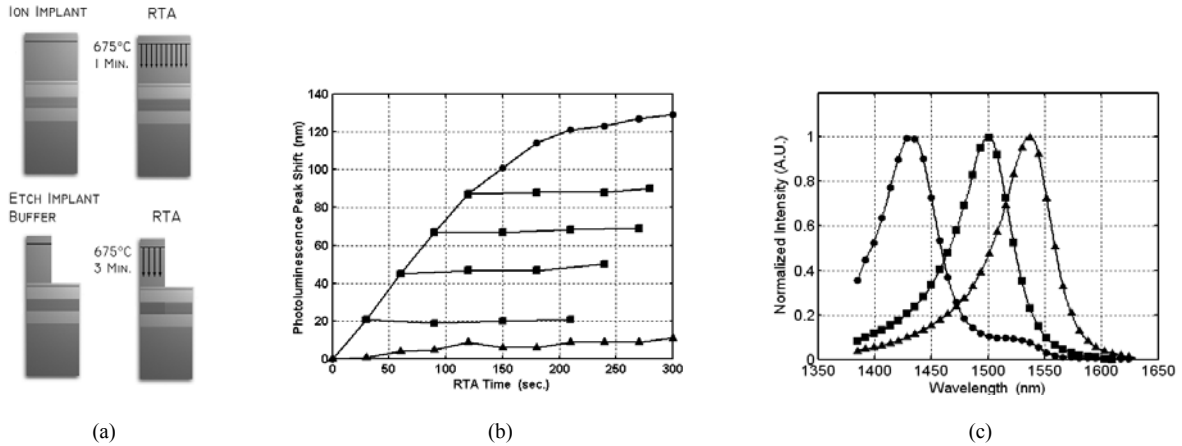


**FIGURE 2.** (a) Illustration of the intermixing processing platform used in this work. (b) Peak photoluminescence peak shift as a function of anneal time, showing the initial linear increase in the peak shift and the complete halting of the peak shift for samples for which the implant buffer layer has been etched. Symbols indicate non-implanted (triangles), implanted (circles), and samples with partial anneal followed by the removal of the implant buffer layer (squares). (c) Photoluminescence spectra for device shown in this work. Symbols indicate active region photoluminescence (triangles), EAM photoluminescence (squares), and passive section photoluminescence (circles).

### 3. PROCESS

The epitaxial base structure, grown on a S-doped InP substrate using a Thomas Swan horizontal-flow rotating-disc MOCVD reactor, contained an n-InP buffer region below a multi-quantum well (MQW) active region centered within a 1.3Q waveguide. The MQW consists of 7 InGaAsP 6.5 nm compressively strained (0.6%) quantum wells, separated by 8.0 nm tensile strained (0.3%) InGaAsP barriers. Following the active region, a 15 nm InP stop etch, a 20 nm 1.3Q stop etch, and a 450 nm InP implant buffer layer was grown.

A 500 nm  $\text{Si}_x\text{N}_y$  mask layer was deposited using plasma enhanced chemical vapor deposition and lithographically patterned such that it remained only where the as-grown band-edge was desired. Ion implantation was performed using  $\text{P}^+$  at an energy of 100 keV, yielding a range of 90 nm, with a dose of  $5\text{E}14 \text{ cm}^{-2}$ , at a substrate temperature of 200 °C [2]. The sample was subjected to rapid thermal processing at a temperature of 675 °C, promoting the diffusion of vacancies through the MQW region. Once the desired band-edge for the EAM was achieved ( $\lambda_{\text{pl}} = 1500 \text{ nm}$ ) the diffusion process was halted. This is accomplished by selectively removing the implant buffer layer, removing the vacancies, thereby halting the intermixing in that region; the regions in which the implant buffer layer remains will continue to intermix along the curve, as shown in Fig. 2b. Using this method, we can achieve multiple band edges across the wafer from a single implant process. The sample was then subjected to an additional rapid thermal anneal, further blue-shifting the regions where the implant buffer layer remained. This second anneal was used to obtain the desired band edge ( $\lambda_{\text{pl}} = 1430 \text{ nm}$ ) for the mirror and passive waveguide sections. A schematic illustrating the intermixing process and the photoluminescence of the active, EAM, and passive regions are shown in Fig. 2a and 2c, respectively.

Once the implant buffer layer was removed, the deeply etched gratings, with a coupling coefficient of  $250 \text{ cm}^{-1}$ , were formed in the DBR region using holography. This was followed by an optimized MOCVD regrowth process of the upper p-cladding and p-type InGaAs contact layer. Ridge waveguides, 3  $\mu\text{m}$  wide, were patterned;  $\text{Si}_x\text{N}_y$  and benzocyclobutene (BCB) were patterned beneath the laser and EAM contacts, respectively. Isolation was accomplished by proton implantation, and p-type metal deposited. The wafers were thinned, backside metalized, and devices were cleaved into bars. Subsequently, the rear facet of cleaved bars was HR-coated.

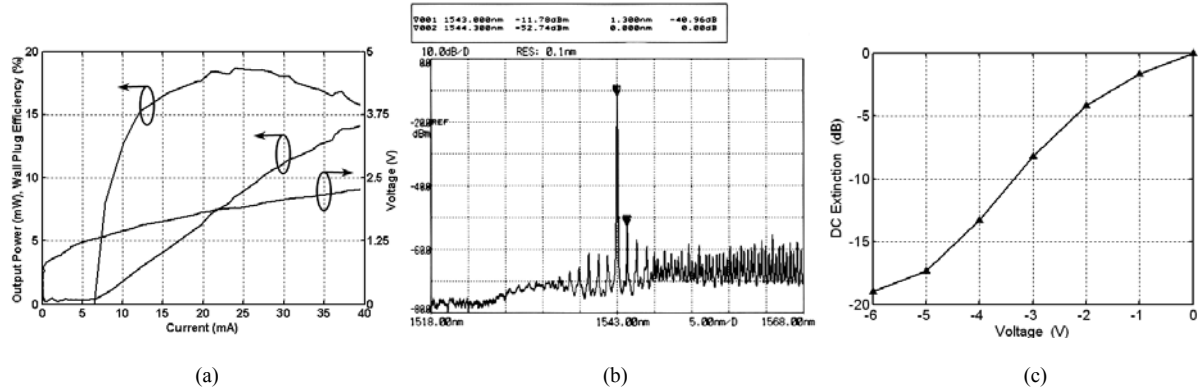


**FIGURE 3.** (a) LIV and wall plug efficiency under pulse testing. (b) CW lasing spectra showing emission at 1543 nm with greater than 40 dB SMSR. (c) DC optical extinction of a 125  $\mu\text{m}$  modulator M1.

#### 4. RESULTS

Material parameters were extracted from all-active and active/passive Fabry-Perot lasers, resulting in a modal gain of  $67\text{ cm}^{-1}$ , an active internal loss of  $9.7\text{ cm}^{-1}$ , and a passive internal loss of  $3.5\text{ cm}^{-1}$  extracted as described in [3]. The power reflectivity of the HR-coating was extracted using all-active Fabry-Perot lasers and found to be  $> 95\%$ . A DBR mirror power reflectivity of 30% was extracted by analysis of DBR laser threshold current and differential efficiency before and after HR-coating.

The devices demonstrated good characteristics in terms of output power, efficiency, side mode suppression ratio (SMSR), and DC optical extinction. A low threshold current of 7 mA was measured, and output powers greater than 10 mW were achieved with a gain section current of 30 mA, as shown in Fig. 3a. The wall plug efficiency exceeded 18% and at 30 mA was 17.5%. The DBR lasers also demonstrated single-mode emission with a SMSR greater than 40 dB, as shown in Fig 3b. The DC modal extinction characteristics of EAM (M1) are presented in Fig. 2c. Greater than 15 dB optical extinction was measured at a reverse bias of 4 V. The laser, at an operating point of 30 mA, had a power dissipation of 50 mW, while the EAM dissipated 30 mW at a reverse voltage of 3.0 V.

#### 5. CONCLUSION

Small footprint, high power laser/modulator devices have been designed, fabricated, and tested. The devices employed a QWI-based processing platform for the monolithic integration of multiple section photonic integrated circuits. Lasers exhibited excellent characteristics in terms of output power ( $>10\text{ mW}$ ) and efficiency ( $> 18\%$ ). The modulator demonstrated  $> 15\text{ dB}$  DC extinction at a length of 125  $\mu\text{m}$ , with expected bandwidth simulated to exceed 15 GHz.

#### 6. REFERENCES

- [1] M. R. Feldman, S. C. Esener, C. C. Guest, and S. H. Lee, "Comparison between optical and electrical interconnects based on power and speed considerations," *Applied Optics*, vol. 27, pp. 1742-1751, 1988.
- [2] E. Skogen, J. Raring, J. Barton, S. DenBaars, and L. Coldren, "Post-Growth Control of the Quantum-Well Band Edge for the Monolithic Integration of Widely-Tunable Lasers and Electroabsorption Modulators," Accepted for publication in *IEEE J. Sel. Topics in Quantum Electron.*, vol. 9, September/October, 2003.
- [3] E. Skogen, J. Barton, S. DenBaars, and L. Coldren, "A Quantum-Well-Intermixing Process for Wavelength-Agile Photonic Integrated Circuits," *IEEE J. Sel. Topics Quantum Electron.* vol. 8, pp. 863-8, 2002.